# Small Molecules of the Month

## September 2022

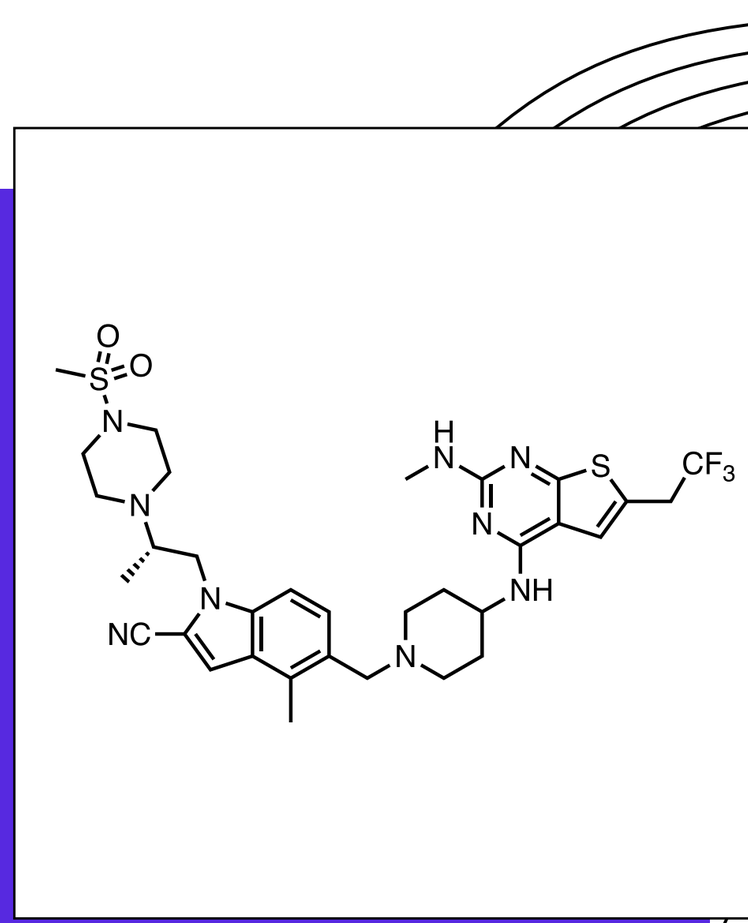


drug hunter

| | | | |
|---|---|---|---|
| 01 | Ziftomenib | Menin-MLL1 PPI | MD Anderson (Kura Oncology) |
| 02 | GB1211 | Galectin-3 | Galecto Biotech |
| 03 | Compound 39 | GCN2 | RAPT Therapeutics |
| 04 | GST-HG131 | PAPD5/PAPD7 | WuXi AppTec |
| 05 | Neflamapimod | p38α kinase | EIP Pharma |
| 06 | AZD1390 | ATM kinase | University of Minnesota (AZ) |
| 07 | Upacicalcet | CaSR | Sanwa Kagaku Kenkyusho Co. |
| 08 | CH7057288 | TRK | Chugai Pharmaceutical Co. |
| 09 | ICeD-2 | DPP9 | Merck & Co. |
| 10 | Vadadustat | PHD | Akebia Therapeutics |

# Ziftomenib

## Menin-MLL1 PPI

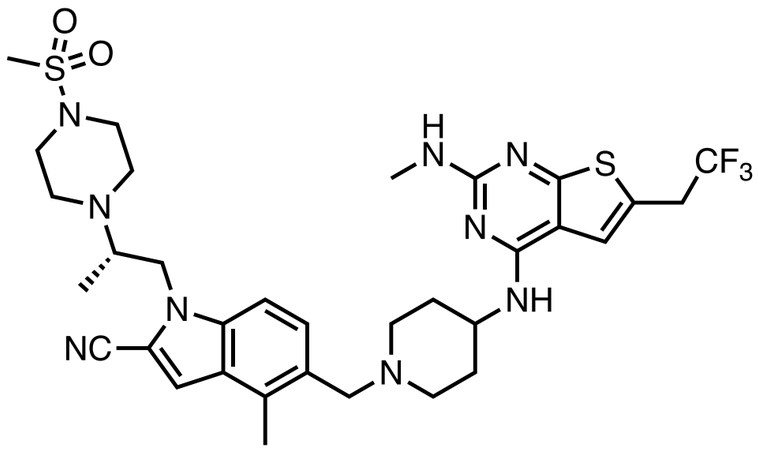


oral menin-MLL1 inhibitor

Ph. I/II candidate in leukemia

from HTS and SBDD

*Leukemia*

Kura Oncology, San Diego, CA

paper DOI: https://doi.org/10.1038/s41375-022-01707-w

**Context.** Ziftomenib (KO-539; MD Anderson) is an oral menin inhibitor being developed for mixed-lineage leukemia 1 (MLL1)-rearranged or *NPM1*-mutated acute myeloid leukemia (AML). Although a tumor suppressor in endocrine glands, the scaffold protein menin is an essential cofactor for leukemogenesis in leukemia subsets driven by the rearrangement of MLL, a histone-lysine methyltransferase, and transcriptional regulator. Based on promising preclinical data and clinical complete responses, inhibitors targeting the MLL1-menin protein-protein interaction (PPI) have potential to become the next novel class of targeted therapy in leukemias, such as AML. Evaluation of synergistic combinations (e.g., w/ BCL-2 inhibitors) involving these menin inhibitors may mitigate the high risk of resistance while offering superior activity.

**Target.** Menin, encoded by the *MEN1* tumor suppressor, is an important cofactor for leukemic cells containing rearrangements in the MLL1 histone methyltransferase complex. Therefore, targeting the menin-MLL1 PPI with menin inhibitors is an emerging novel therapeutic strategy for MLL1-rearranged AML. In addition to MLL1-rearranged AML leukemic cells, menin inhibitors also inhibit *NPM1*-mutated leukemias, which are characterized by aberrant cytoplasmic retention of the encoded nucleophosmin. Several menin inhibitors have been described, and at least two are in clinical development (KO-539 and SNDX-5613).

**Mechanism of Action.** The menin-MLL1 interaction involves two MLL1 peptide fragments nested within the large (5000 [3]), rigid cavity of menin, making it a challenge to develop potent and selective molecules. First generation menin inhibitors required high (>2 μM) concentrations to repress gene expression and exhibited modest effects in mouse models, but University of Michigan scientists developed a second generation inhibitor, MI-3454, a structurally related molecule to ziftomenib, that binds menin's cavity with a high degree of shape complementarity with nanomolar activity.

**Hit-Finding Strategy.** A high-throughput screen of 49,000 compounds from the Center for Chemical Genomics at the University of Michigan identified MI-1 ($IC_{50}$ = 1.9 μM) as an initial hit. The HTS involved a stepwise procedure, including two fluorescence polarization assays with menin and fluorescein- and Texas Red-labeled MLL-derived peptide containing the high-affinity menin binding motif (MBM1), followed by validation of menin binding by the identified compounds. MI-1 is a reversible inhibitor of the menin-MLL interaction, based on saturation transfer difference NMR experiments.

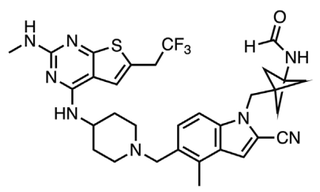


**MI-3454**

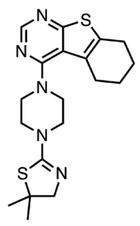


**MI-1**
FP $IC_{50}$ = 1.9 μM

# Ziftomenib

## Menin-MLL1 PPI

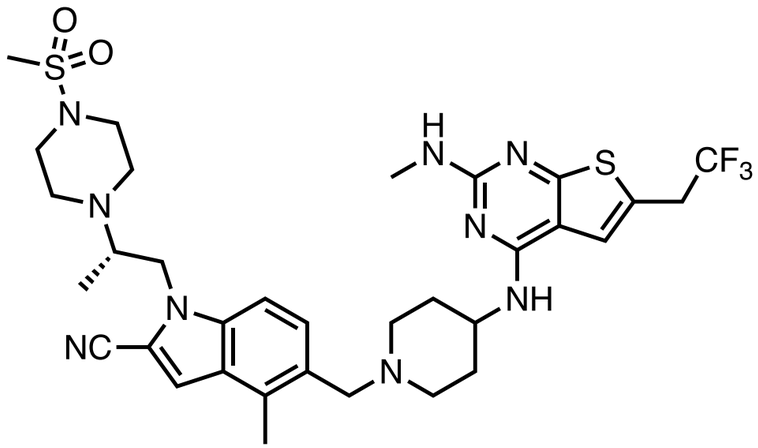

oral menin-MLL1 inhibitor

Ph. I/II candidate in leukemia

from HTS and SBDD

*Leukemia*

Kura Oncology, San Diego, CA

paper DOI: https://doi.org/10.1038/s41375-022-01707-w

drug hunter

**Lead Optimization.** A structure-activity relationship study, based on MI-1, and structure-based design identified a trifluoroethyl substituent on the thienopyrimidine ring that improved potency by >40 fold (MI-2-2, FP $IC_{50}$ = 46 nM, ITC $K_d$ = 22 nM). To improve the cellular activity and metabolic stability of MI-2-2, further structure-guided design together with traditional medicinal chemistry efforts identified a modified molecular scaffold, leading to MI-463 (FP $IC_{50}$ = 15 nM, ITC $K_d$ = 10 nM) and MI-503 (FP $IC_{50}$ = 15 nM, ITC $K_d$ = 9 nM). With >2 fold potency increase, the molecules also show high oral bioavailability (in mice, F = 44% for MI-463, 73% for MI-503), selective on-target activity in MLL leukemia cells ($GI_{50}$ = 0.23 µM, 0.22 µM for MI-463, MI-503), and substantial improvement of survival in a MLL- leukemia mouse model (median survival = 70%, 45% for MI-463, MI-503). In the patent WO2017161028A, ziftomenib showed a potency of $IC_{50}$ <50 nM (with menin and a peptide containing the high affinity menin binding motif found in MLL in an FP assay) and $GI_{50}$ <10 nM (in MLL-AF9 bone marrow cells).

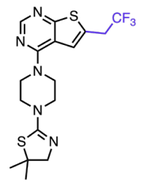

**MI-2-2**
FP $IC_{50}$ = 46 nM
ITC $K_d$ = 22 nM

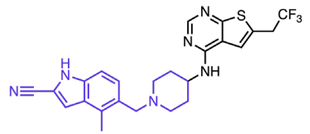

**MI-463**
FP $IC_{50}$ = 15 nM
ITC $K_d$ = 10 nM

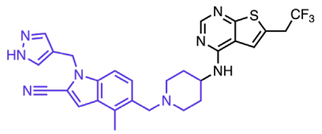

**MI-503**
FP $IC_{50}$ = 15 nM
ITC $K_d$ = 9 nM

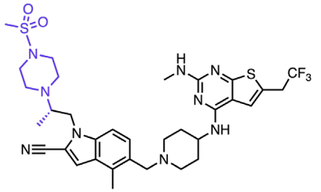

**ziftomenib**
FP $IC_{50}$ <50 nM
$GIC_{50}$ < 10 nM

**Binding Mode.** The binding mode of ziftomenib is not yet disclosed. However, the crystal structures of close analogs show that these compounds can compete with MLL1 in the menin binding site inhibiting menin-MLL1 interaction. Crystal structures of MI-503 (**PDB:4X5Y**), MI-1481 (**PDB:6BXY**), and MI-3454 (**PDB:6O5I**) in complex with menin exemplify the binding mode.

**Preclinical Pharmacology.** Ziftomenib demonstrated menin inhibition in several cell models, including depleting menin, MEF2C, MEIS1, FLT3, CDK6 and BCL2 expression in MOLM13 and OCI-AML3 cells and altering MLL1 target gene expressions in patient-derived AML stem cells with high expression of genes commonly implicated in AML, including CD123 and CD33. In NSG mice engrafted with patient-derived AML stem cells harboring MLL1-r and FLT3-TKD mutations, ziftomenib decreased AML burden and improved AML survival. Co-treatment of ziftomenib and the BCL-2 inhibitor, venetoclax, which is approved for the treatment of AML in combination with chemotherapy or a hypomethylating agent, showed a synergistic effect in both patient-derived AML stem cells harboring a mtNPM1 or mtNPM1/mtFLT3 mutation and in the mouse model of AML. Ziftomenib's in vitro and in vivo activity was also tested in combination with OTX015, an investigational BET inhibitor that induces down-regulation of CDK6, and showed a similar synergistic effect, improving in vivo AML survival.

**Clinical Development.** Ziftomenib is currently being evaluated in a Ph. I/II (NCT04067336) dose-escalation and dose-validation/expansion study in patients with relapsed or refractory AML. Preliminary data showed that currently enrolled patients studied for safety (n=3) had not exhibited any dose-limiting toxicities at the data cutoff, and no treatment-related deaths were reported.

**Patent.** The University of Michigan has patented several menin-MLL inhibitor series in past years. Ziftomenib and analogs were described in the patent WO2016195776A1. The US patent US10174041B2 was granted to the University of Michigan and Kura Oncology Inc. in January 2019, and is valid until March 2036.

# GB1211

## Galectin-3

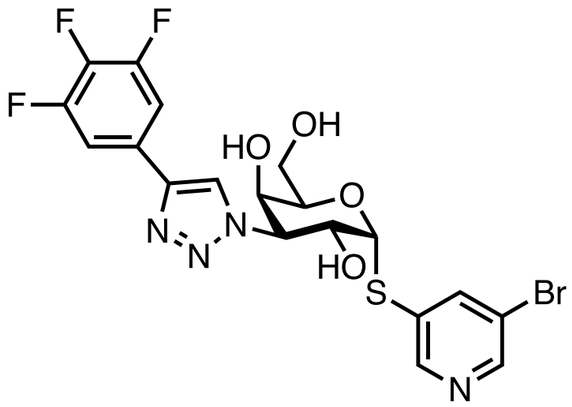


oral galectin-3 inhibitor

Ph. I/II candidate in cancer and liver diseases

LLE and PK opt. from a prev. clinical candidate

*J. Med. Chem.*

Galecto Biotech, Gothenburg, SE

paper DOI: https://doi.org/10.1021/acs.jmedchem.2c00660

**Context.** GB1211 (Galecto Biotech) is an oral galectin-3 inhibitor under development for fibrotic disease. First described in 1971, galectin-3, a unique subtype of a 15-member family of carbohydrate-binding proteins, has been implicated in a host of different diseases, such as cancer, liver cirrhosis, and atherosclerosis. Incredibly, over 8000 papers featuring the protein have since been published. Despite the promise for drug discovery, key liabilities such as low affinity and/or limited bioavailability have precluded the clinical success of previously described galectin-3 inhibitors, challenges Galecto Biotech are hoping to overcome. GB1211, the flagship compound of a new class of α-D-monogalactopyranoside with nanomolar affinity and improved oral bioavailability, demonstrated promising preclinical efficacy and is currently in early clinical development for liver fibrosis and lung cancer.

**Target.** Galectins are a large 15-member family of glycan-binding proteins that mediate several pathophysiological processes, such as immune and inflammatory responses, tumorigenesis/progression, neural degeneration, and metabolism. Galectin-3, a key galectin, is ubiquitously-expressed and regulates important cellular functions such as growth, proliferation, differentiation, and inflammation. In animal studies, deficiency of galectin-3 or pharmacological inhibition of the protein was found to protect mice from fibrosis. However, fibrotic tissues of patients with chronic liver disease expressed significantly higher levels of galectin-3.

**Mechanism of Action.** GB1211 is a member of a new class of α-D-monogalactopyranosides and binds with nanomolar affinity to a shallow, amphiphilic pocket in galectin-3, which was previously targeted by β-D-galactopyranosides (e.g., "compounds 14" and "53") or thiodigalactosides (e.g., "compounds 24" and "85") that had low affinity and/or limited bioavailability. Using crystallographic analysis, Galecto scientists determined that the α-aglycon of this new inhibitor class made novel interactions with the galectin-3 site that increased affinity by five orders of magnitude compared to galactose (**PDB:6EOG;6EOL**).

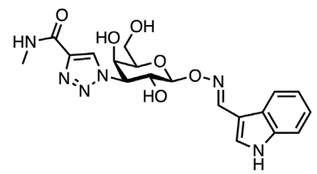

**compound 14**
$K_d$ = 11 μM

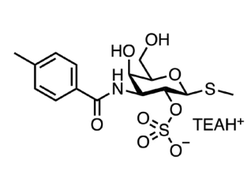

**compound 53**
$K_d$ = 87 μM

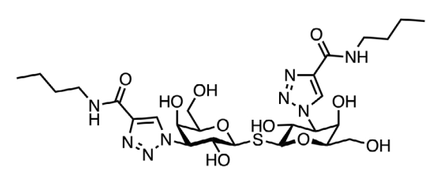

**compound 24**
$K_d$ = 0.029 μM

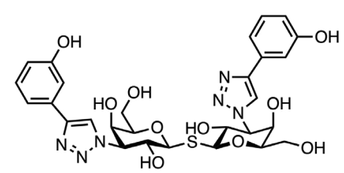

**compound 85**
$K_d$ = 0.013 μM

**Hit-Finding Strategy.** GB0139 was identified as a promising inhibitor of galectin-3 ($K_d$ = 2.3 nM) using a competitive fluorescence anisotropy assay to detect protein binding out of a library of 16 thiodigalactosides. The aryl-triazolyl and fluorine substitutions are essential moieties for high-affinity binding. This thiodigalactoside is currently under Ph. IIb evaluation as an inhaled therapy for idiopathic pulmonary fibrosis and was selected as the starting point for lead optimization to improve oral bioavailability.

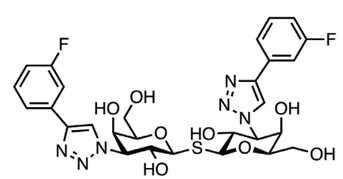

**GB0139**
Galectin-3 $K_d$ = 2.3 nM

# GB1211

## Galectin-3

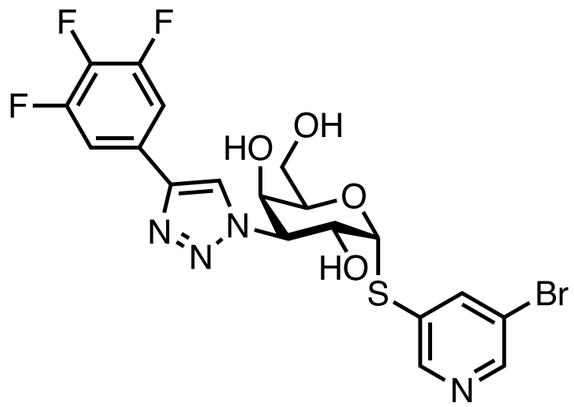

oral galectin-3 inhibitor

Ph. I/II candidate in cancer and liver diseases

LLE and PK opt. from a prev. clinical candidate

*J. Med. Chem.*

Galecto Biotech, Gothenburg, SE

paper DOI: https://doi.org/10.1021/acs.jmedchem.2c00660

drug hunter

**Lead Optimization.** Enhancing cell permeability was the primary goal of this optimization campaign. Starting with GB0139, a small library of thiodigalactosides was synthesized to improve bioavailability by masking or removing hydroxyl groups. Despite modest improvements in permeability, the masked thiodigalactosides suffered from poor affinity (e.g., >100 µM). Correlation between high permeability ($P_{app}$) and low polar surface area (PSA) from Galecto's in-house library led to the investigation of a class of 1,3-disubstituted β-D-monogalactopyranosides, including "compound 8c," which showed improved permeability (30/29 $10^{-6}$ cm/s) and a promising $K_d$ (5.2 µM). To further improve affinity for galectin-3, the anomeric center was switched from the β-configuration to α in a new series of compounds as previously demonstrated, leading to GB1211 with nanomolar affinity for galectin-3 (25 nM), promising bioavailability in mice (68%), and low hERG liability (> 10 µM).

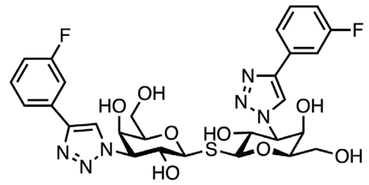

**GB0139**
galectin-3 $K_d$ = 2.3 nM
$P_{app}$ (CACO-2) = 0.07/0.05 $10^{-6}$ cm/s
PSA = 210 Å²

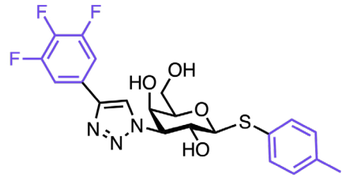

**compound 8c**
galectin-3 $K_d$ = 5.2 µM
$P_{app}$ (CACO-2) = 30/29 $10^{-6}$ cm/s
PSA = 101 Å²

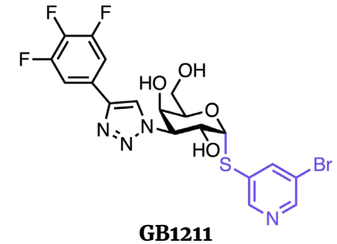

**GB1211**
galectin-3 $K_d$ = 25 nM
$P_{app}$ (CACO-2) = 4.6/30 $10^{-6}$ cm/s
PSA = 114 Å²

**Binding Mode.** The co-crystal structure of GB1211 complexed with human galectin-3C (**PDB:7ZQX**) in the carbohydrate-recognition domain shows several interactions between the protein environment and the thiogalactoside core. Other relevant interactions include the halogen bond between the bromine atom and Gly182 residue and stacking interactions between the phenyltriazoyl moiety and Arg144 residue.

**Preclinical Pharmacology.** Through a number of cellular assays, GB1211 was found to have low cell cytotoxicity in an MTT (3-[4,5-dimethylthiazol-2-yl]-2,5 diphenyltetrazolium bromide) assay, functionally inhibit galectin-3 in human monocyte THP1 cells, and inhibit TGFβ-induced expression of Col1A2, α-SMA, TIMP1, and LGalS3, which are genes implicated in fibrosis, in human liver stellate cells (LX2). In mice with $CCl_4$-induced liver fibrosis, blockade of galectin-3 by GB1211 significantly reduced fibrotic collagen deposition in the hepatic parenchyma, determined by picrosirius red (PSR) staining. In mice treated with bleomycin to induce pulmonary fibrosis, GB1211 significantly reduced collagen deposition in the lungs. Due to the lower affinity for mouse galectin-3 ($K_d$ = 0.77 µM) than the human protein ($K_d$ = 0.025 µM), the in vivo experiments required high doses of GB121 (up to 10 mg/kg BID).

**Clinical Development.** In a completed Ph. I safety and tolerability study (NCT03809052), GB1211 was found to be well tolerated, and had no serious adverse events or deaths. A Ph. I/II study (NCT05240131) evaluating the drug in combination with atezolizumab, an anti-PD-L1 antibody approved for metastatic non-small cell lung cancer (NSCLC) with high PD-L1 expression, in patients with NSCLC is currently underway. Galectin-3 is a marker of resistance to checkpoint inhibitors in patients with NSCLC, and in animal models, galectin-3 and immune checkpoint inhibitors have a synergistic effect, therefore co-administration of a galectin-3 inhibitor with a checkpoint inhibitor-based immunotherapy, like atezolizumab, is hypothesized to enhance the immune response and overcome checkpoint inhibition resistance.

**Patent.** GB1211 and other α-D-galactoside analogs were disclosed in the patent WO2016120403A1.
The US patent US11377464B2 was granted to Galecto Biotech AB in September 2020, and is valid until January 2036.

# Compound 39

## GCN2

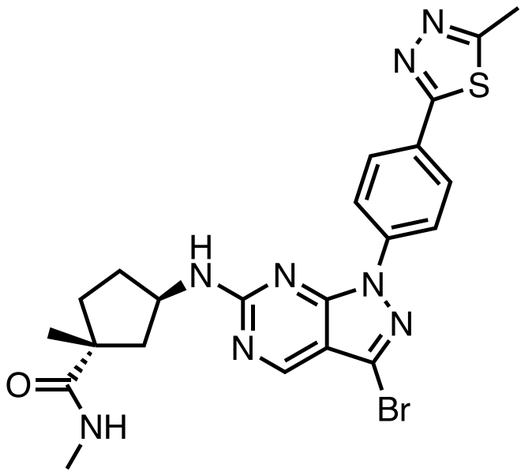


oral GCN2 kinase inhibitor

TGI in LL2 syngeneic mouse model

SAR opt. from literature starting point

*J. Med. Chem.*

RAPT Therapeutics, South San Francisco, CA

paper DOI: https://doi.org/10.1021/acs.jmedchem.2c00736

**Context.** "Compound 39" (RAPT Therapeutics) is a general control nonderepressible 2 (GCN2) protein kinase inhibitor. As the master regulator of the integrated stress response triggered by cellular stress in the tumor microenvironment, GCN2 has been implicated in tumor progression and immune escape, making the kinase an attractive oncotarget. Notably, GCN2 expression triggers the activation of myeloid-derived suppressive cells (MDSCs), which have been associated with T cell suppression and poor prognosis in cancer patients. Targeting GCN2 presents a novel approach to inhibiting MDSCs-mediated immune suppression. However, skeptics of this approach, backed by findings from an in vivo mechanistic study, speculate that systemic targeting of GCN2 may harm the expression of specific immune cells, such as CD8+ T-cells. In an in vitro assay, "compound 39" at 600 nM prevented MDSC-induced suppression of the proliferation of co-cultured CD8+ T cells, suggesting that the compound may restore cytotoxic T cell expression rather than hamper it. Additional in vivo data will help ascertain the promise of this class of anticancer compounds, and this molecule may be a valuable tool to help understand this target.

**Target.** GCN2, a ubiquitously expressed serine/threonine protein kinase, is regarded as the master regulator of amino acid homeostasis in the cell. Tumor microenvironment (TME)-induced cellular stress triggers activation of GCN2, which triggers the expression of stress-related transcription factors. Importantly, activation of GCN2 contributes to suppression of T cell expression in the TME mediated by MDSCs. Reports have identified GCN2 as important for tumor cell survival in the TME. Furthermore, MDSCs, which are known to preclude cytotoxic T-cell proliferation, have been associated with poor clinical outcomes and immunotherapy resistance in cancer patients.

**Mechanism of Action.** Based on computational docking, the selective inhibitory activity of "compound 39" is thought to be due to its specific fit into the active site of GCN2, which has an unusual phenylalanine (Phe855) at the pocket bottom that is commonly occupied by valine or leucine in other kinases. "Compound 39" exhibited at least 20-fold to over 10,000-fold selectivity for GCN2, as assessed using the KinaseProfiler platform at Eurofins Discovery.

**Hit-Finding Strategy.** "Compound 1," a non-selective kinase inhibitor identified in a series of Merck KGaA patents, was used as the starting point in this study. This compound and other triazolopyrimidine-containing molecules were reported to display nanomolar potency against GCN2 along with other targets (e.g., "compound 1", $^{33}$P-ATP $IC_{50}$ = 19 nM (GCN2), 40 nM (PKR)).

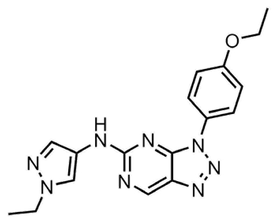


**Compound 1**
$^{33}$P-ATP $IC_{50}$ = 19 nM (GCN2),
40 nM (PKR)

# Compound 39

## GCN2

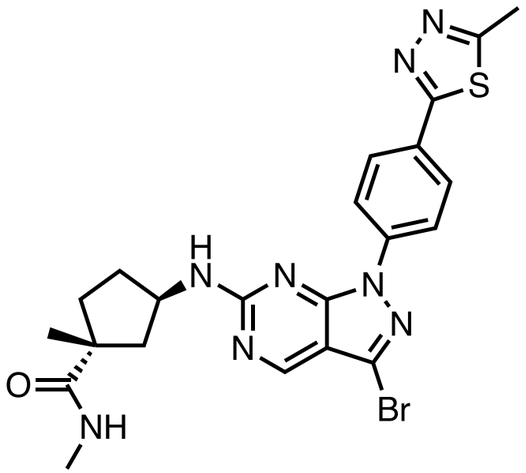

oral GCN2 kinase inhibitor

TGI in LL2 syngeneic mouse model

SAR opt. from literature starting point

*J. Med. Chem.*

RAPT Therapeutics, South San Francisco, CA

paper DOI: https://doi.org/10.1021/acs.jmedchem.2c00736

**Lead Optimization.** To alleviate strong off-target inhibition and to improve the solubility of "compound 1", rounds of SAR studies were carried out to sequentially modify the heterocyclic core and substituents. The addition of bromine to the pyrazolopyrimidine core, as well as the replacement of the *para*-ethoxyphenol with a quinoline moiety and the ethyl-pyrazole with a piperidinyl-pyrazole led to "compound 19" and a > 6-fold increase of in vitro potency (TR-FRET $IC_{50}$ = 3 nM, SKOV-3 cellular $IC_{50}$ = 610 nM), but at the cost of poor cellular permeability and kinome selectivity. To solve these issues, further optimization on the same bromopyrazolopyrimidine core led to the discovery of "compound 37", which replaced the piperidinyl-pyrazole with a cyclopentylamine pendant. This molecule exhibited improved cellular potency (TR-FRET $IC_{50}$ = 17 nM, SKOV-3 cellular $IC_{50}$ = 21 nM) and a good rat PK profile (CL = 8.0 mL/min/kg, PO AUC = 1512 h*ng/mL, %F = 36). However, recognizing that the 2,3-unsubstituted quinoline group may impose a mutagenicity risk, alternative substituents were searched, leading to "compound 39". "Compound 39" proved to possess high potency (TR-FRET $IC_{50}$ = 5 nM, SKOV-3 cellular $IC_{50}$ = 16 nM), desired rat PK profile (CL = 5.9 mL/min/kg, PO AUC = 4598 h*ng/mL, %F = 80%), and at least >20-fold selectivity over >400 off-target kinases.

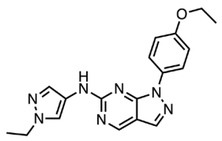

**compound 1**
$^{33}$P-ATP $IC_{50}$ = 19 nM

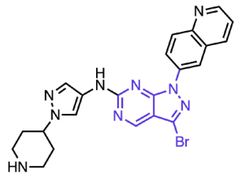

**compound 19**
TR-FRET $IC_{50}$ = 3 nM
SKOV-3 $IC_{50}$ = 610 nM

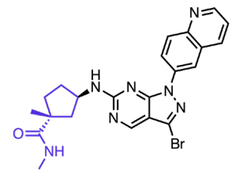

**compound 37**
TR-FRET $IC_{50}$ = 17 nM
SKOV-3 $IC_{50}$ = 21 nM
%F = 36

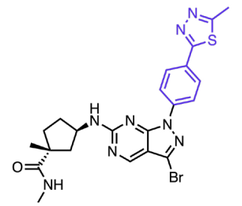

**compound 39**
TR-FRET $IC_{50}$ = 5 nM
SKOV-3 $IC_{50}$ = 16 nM
%F = 80

**Binding Mode.** The crystal structure of GCN2 complexed with "compound 39" was not published. However, through docking models, the authors suggest that "compound 39" binds in the ATP-binding site of the kinase domain, similar to the previously disclosed Takeda GCN2 inhibitor "compound 6d". An interesting observation concerns the presence of Phe855 residue at the bottom of the pocket site. The presence of this residue can explain some SAR study results, as the potency decrease resulting from ortho-substitution in the phenyl ring, which is possibly due to the steric clashes in this site.

**Preclinical Pharmacology.** GCN2 inhibition by "compound 39" relieved MDSC-mediated T cell suppression in a mouse model of pancreatic cancer. The effect of "compound 39's" inhibition on MDSC suppression of T cell proliferation was similar to that of the same model implemented in GCN2 knockout mice. As MDSC-mediated T cell suppression is a mechanism of tumor immune escape and homeostasis, these results demonstrate that GCN2 inhibition can disrupt the TME. "Compound 39" (50 mg/kg BID for 26 days) inhibited tumor growth (56% vs. vehicle) in a syngeneic mouse model of lung carcinoma with activated GCN2 and high MDSC presence, demonstrating therapeutic potential. The expression of vascular endothelial growth factors (VEGF) is associated with increased presence of T cells and MDSCs, limiting the effect of anti-VEGF agents in tumors with high MDSC presence. Further, there is a reported mechanism for GCN2/ATF4 regulation of VEGF to trigger angiogenesis in the presence of amino acid restriction. "Compound 39" was tested in combination with an anti-VEGFR antibody, to show an expected synergistic effect (79% tumor growth inhibition vs. vehicle).

**Clinical Development.** Preclinical compound.

**Patent.** RAPT Therapeutics' pyrozolo-pyrimidin-amino-cycloalkyl compounds series for the treatment of cancer was described in patent WO2019236631A1. The US patent US11046699B2 was granted in June 2021, and is valid until June 2039.

# GST-HG131

## PAPD5/PAPD7

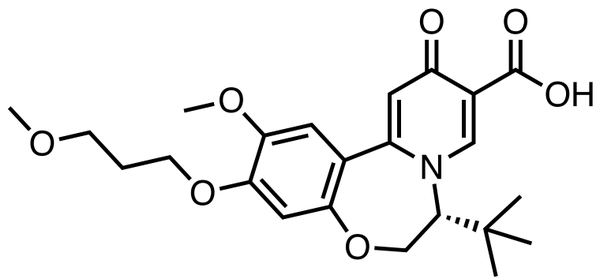


oral HBV antigen inhibitor

Ph. I candidate for hepatitis B

SAR opt. of a previously disclosed inhibitor

*Bioorganic Med. Chem. Lett.*

WuXi AppTec, Shanghai, CN

paper DOI: https://doi.org/10.1016/j.bmcl.2022.128977

**Context.** GST-HG131 (WuXi AppTec) is an oral hepatitis B virus (HBV) inhibitor which lowers hepatitis B antigen (HBsAg) levels which entered clinical development in Chinese subjects for chronic hepatitis B infection. Despite the significant research strides made in the elucidation of the biology of HBV, chronic HBV infection continues to remain a significant global health challenge, with functional cure rates of current treatments at <30%. Although no current treatment eradicates the virus, there is an effective vaccine available to prevent infection. One potential reason why new HBV therapies are often tested in China is that the adult vaccination rate there is only 26%.

HBV antigen loss and seroconversion are key endpoints of chronic HBV treatment, and HBsAg itself can suppress immunity, making drugs that lower HBsAg levels attractive. GST-HG131 leads a series of dihydrobenzopyridooxazepine compounds developed from a previous agent with a novel mechanism of action, Roche's RG7834 (RO7020322), which selectively reduces HBsAg and HBeAg levels. Although the development of RG7834 seems to have been terminated, WuXi AppTec scientists suspect that this is due to safety issues, hope to advance GST-HG131 further. Preliminary results from a Ph. I study in healthy subjects show that the drug was found to be tolerable and generally safe up to multiple doses of 60 mg and below, which may reach needed coverage requirements.

**Target.** Although there is no definitive cure for HBV, one of the primary goals of treatment is viral suppression measured by loss of serum viral surface antigen (HBsAg). Reduction of HBsAg levels can lead to patients being considered "functionally cured." Several clinical studies evaluating inhibitors focused on reducing HBV antigen levels have been reported. GST-HG131 reduces levels of HBeAg and HBsAg, which is a marker for developing chronic liver disease and hepatocellular carcinoma. The specific target and mechanism of antigen reduction for many agents, are unclear, but interaction with RNA polymerases PAPD5 and PAPD7 is likely based on in vitro studies of RG7834.

**Mechanism of Action.** GST-HG131 is structurally based on Roche's dihydroquinolizinone clinical candidate RG7834 which uses a novel MoA involving the reduction of viral mRNAs via inhibition of the host's non-canonical poly(A) RNA polymerases, PAPD5 and PAPD7 - unlike nucleoside/nucleotide inhibitors that act on the viral DNA polymerase.

**Hit-Finding Strategy.** The program started from Roche's first-in-class clinical candidate RG7834 (RO7020322), with a focus on improving the pharmacokinetic activity and safety profile in rodents.

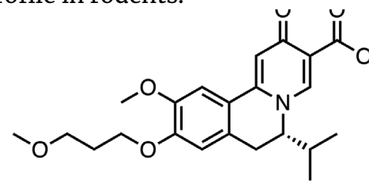


**RG7834**
HBV-DNA $EC_{50}$ = 0.8 nM
HBsAg $EC_{50}$ = 1.1 nM

# GST-HG131

## PAPD5/PAPD7

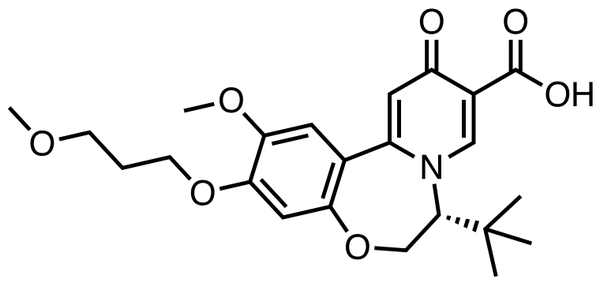

oral HBV antigen inhibitor

Ph. I candidate for hepatitis B

SAR opt. of a previously disclosed inhibitor

*Bioorganic Med. Chem. Lett.*

WuXi AppTec, Shanghai, CN

paper DOI: https://doi.org/10.1016/j.bmcl.2022.128977

**Lead Optimization.** RG7834 clinical studies were halted during Ph. I, however no official reason was provided. Lead optimization began with a different dihydroquinolizinone (DHQ) "compound 1," as the structure of RG7834 was not disclosed at the time, with a focus on retaining potency while optimizing the safety profile. A library of dihydrobenzopyridooxazepines (DBP) was designed to preserve known pharmacophores within "compound 1" and assess SAR at *C*-7 position. "Compound 3h" exhibited the most promising antiviral activity within the series with the installation of a *t*-butyl group and expansion of the isoquinoline ring into a benzoxazepine. However, this was a poor candidate for oral administration. Substituting the *C*-2 chlorine for a lipophilic methoxy group reduced the cLogD from 4.3 to 3.4 for GST-HG131, which retained single-digit nanomolar antiviral activity and dramatically improved oral exposure ($C_{max}$ = 1055 nM, 2 mg/kg PO, mice) and bioavailability (%F = 92%) in multiple animal species.

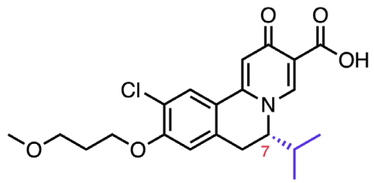

**"compound 1"**
HBV-DNA $EC_{50}$ = 0.8 nM
HBsAg $EC_{50}$ = 0.9 nM

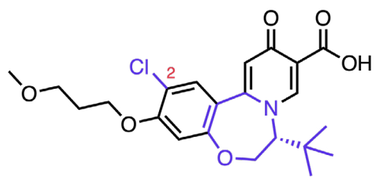

**"compound 3h"**
HBV-DNA $EC_{50}$ = 0.5 nM
HBsAg $EC_{50}$ = 0.7 nM
ClogP = 4.3
$C_{max}$ (PO, mice) = 203 nM
%F = 18%

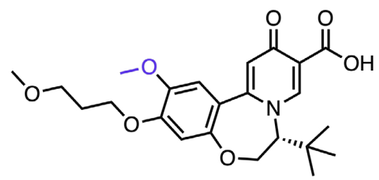

**GST-HG131**
HBV-DNA $EC_{50}$ = 2.6 nM
HBsAg $EC_{50}$ = 3.9 nM
ClogP = 3.4
$C_{max}$ (PO, mice) = 1055 nM
%F = 92%

**Binding Mode.** Structure not disclosed.

**Preclinical Pharmacology.** To elucidate its mechanism of action, GST-HG131's effect on HBV RNA levels was evaluated in human hepatocytes expressing HBV compared with entacavir, an FDA approved treatment for HBV that acts as a HBV nucleoside reverse transcriptase inhibitors. As expected, GST-HG131 exhibited a dose- and time-dependent inhibition of HBV RNAs, with entacavir having no effect on HBV RNAs. In a mouse model of HBV, GST-HG131 demonstrated dose-dependent reduction of HBsAg and HBeAg, to a similar magnitude as RG7834. The effect was also similar to that of tenofovir disoproxil fumarate, which is an FDA approved treatment for chronic HBV and acts as a nucleotide analog reverse-transcriptase inhibitor. Of note, the combination of GST-HG131 with tenofovir disoproxil fumarate did not significantly improved HBsAg and HBeAg reductions. In rat toxicology studies comparing GST-HG131 and RG7834, both drugs had similar tolerability at low (100 mg/kg) and medium (300 mg/kg) doses, however at the highest dose tested (1000 mg/kg) RG7834 showed more organ abnormalities. The medium and high doses of RG7834 also exhibited mydriasis (pupil dilation) and low rectal temperatures, suggesting that GST-HG131 may have better tolerability.

**Clinical Development.** The compound is currently being evaluated in a Ph. I safety, tolerability and pharmacokinetic study (NCT04499443) with dose-expansion. Preliminary results from the study suggested that single doses ≤ 300 mg and multiple doses ≤ 60 mg were generally well-tolerated and safe. In the single-dose study, $t_{max}$ was 1-6 h and $t_{1/2}$ was 3.9-14.3 h.

**Patent.** The dihydrobenzopyridooxazepine Fujian Akeylink Biotechnology HBV antigen inhibitor series was described in the patent WO2018161960A1. The US patent US11008331B2 was granted in May 2021, and is valid until April 2038.

# Neflamapimod

## p38α kinase

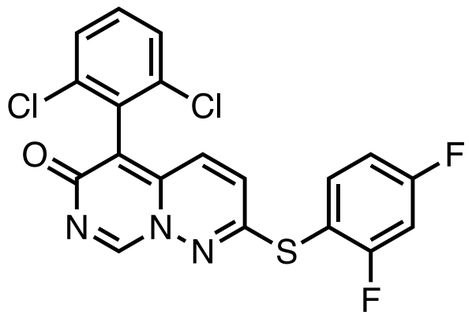


oral p38α kinase inhibitor

Ph. II candidate in neurology

from SBDD and opt.

*Nat. Commun.*

EIP Pharma Inc, Boston, MA / Vertex, Cambridge, MA

paper DOI: https://doi.org/10.1038/s41467-022-32944-3

**Context.** Neflamapimod (EIP Pharma, VX-745) is an oral, brain-penetrant p38α kinase inhibitor under development for neurodegenerative disorders. Among the roles of p38α MAPK is the activation of Rab5, a small endosome-associated Ras GTPase that regulates intracellular trafficking pathways. This, coupled with the involvement of Rab5 in the molecular mechanisms leading to the degeneration of basal forebrain cholinergic neurons (BFCNs), led to the hypothesis that inhibiting p38α could be a therapeutic strategy for diseases associated with BFCN dysfunction, such as dementia with Lewy bodies (DLB). Supported by mouse data, neflamapimod, likely the most advanced p38α MAPK inhibitor, has since progressed to clinical development, and two Ph. II studies have been completed (NCT03402659 and NCT04001517). Although data from the REVERSE-SD study in patients with mild Alzheimer's disease did not point to a neflamapimod-mediated improvement in episodic memory, results from the AscenD-LB study in patients with DLB showed that the drug has disease-modifying potential.

**Target.** The ubiquitously expressed Ras GTPase Rab5 is a major regulator of the preliminary steps of endocytosis and subsequent endosomal membrane trafficking, sorting, and endosomal fusion. Hyperactivation of Rab5 in mice was found to be associated with basal forebrain cholinergic neuron (BFCN) degeneration, a crucial driver of neurodegenerative dementia. A key regulator of Rab5 activity is p38α MAPK, and the first study to demonstrate this link was described two decades ago.

**Mechanism of Action.** The mechanism of reducing inflammation in the CNS through p38α kinase inhibition is believed to be through reducing cytokine production. Interestingly, neflamapimod's MoA likely involves inhibition of IL-1β cytokine signaling rather than IL-1β production as the dose required to demonstrate cognitive improvement (1.5 mg/kg in mice by the water maze test) or better functional mobility (40 mg BID for patients < 80 kg and 40 mg TID for ≥ 80 kg in a Ph. II trial) was lower than the dose required to reduce IL-1β levels.

**Hit-Finding Strategy.** A combination of virtual screening and shape similarity methods were first used to screen commercial compounds with similar configurations but differing connectivity compared to early tool "compound 2", which binds to p38α in the ATP-binding pocket but causes inhibition of cytochrome P450 enzymes. The initially proposed hit structure ("compound 4", based on proposed vendor structure) emerged in subsequent screening using a coupled spectrophotometric assay, in which ADP generated by a kinase is converted to ATP by a coupled assay resulting in a reduced NADH readout signal.

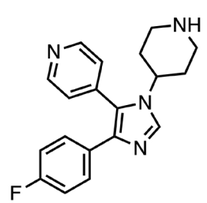


**compound 2**

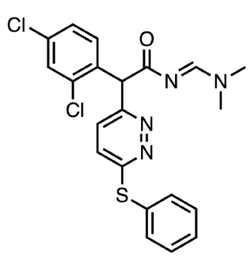


**compound 4**

# Neflamapimod

## p38α kinase

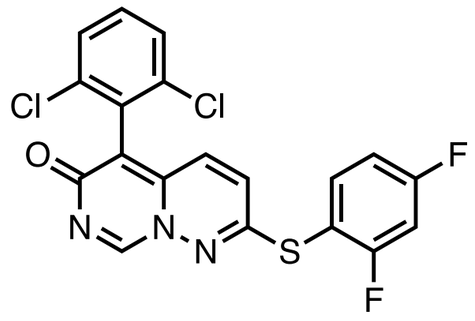


oral p38α kinase inhibitor

Ph. II candidate in neurology

from SBDD and opt.

*Nat. Commun.*

EIP Pharma Inc, Boston, MA / Vertex, Cambridge, MA

paper DOI: https://doi.org/10.1038/s41467-022-32944-3

drug hunter

**Lead Optimization.** During an in-house attempt to resynthesize proposed hit structure of "compound 4," "compound 10", containing an unreported bicyclic core, was obtained. This unusual core was postulated to result from ring closure of *in situ*-generated "compound 4." With the promising potency of "compound 10" ($IC_{50}$ = 5 µM (p38α), 20 µM (PBMC IL-1β), 20 µM (PBMC TNFα)), SAR studies were carried out on the two substituents of the bicyclic core. Migration of the phenyl chlorine in the para-position to the ortho-position and the addition of a *para* and *ortho* fluorine to the thiophenol moiety led to the discovery of neflamapimod. Neflamapimod demonstrates >550-fold improved inhibition against p38α ($IC_{50}$ = 9 nM), >20 fold selectivity over p38β ($K_i$ = 220 nM), no significant inhibition towards >50 MAP and other kinases, favorable PK profile (mouse CL = 21 mL/min/kg, PO AUC = 26.96 h*µg/mL, %F = 87%), and anti-inflammatory effect in a mouse model. The impact of three halogen atoms on overall compound properties is remarkable.

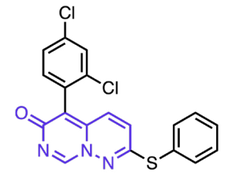


**compound 10**
Coupled assay $IC_{50}$ = 5 µM (p38α),
20 µM (PBMC IL-1β),
20 µM (PBMC TNFα)

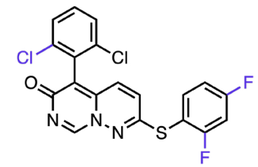


**neflamapimod**
Coupled assay $IC_{50}$ = 9 nM (p38α),
45 nM (PBMC IL-1β),
51 nM (PBMC TNFα),
%F = 87%

**Binding Mode.** The crystal structure of neflamapimod in complex with p38α (**PDB:3ZSI**) reveals a flipped glycine in the protein hinge region. The difluorophenyl and dichlorophenyl moieties occupy hydrophobic pockets, and the carbonyl oxygen forms hydrogen bonding interactions with Gly110 and Leu108 residue. Interestingly, the DFG motif in the ATP binding site adopts an unusual DFG-out conformation.

**Preclinical Pharmacology.** In a transgenic mouse model of down syndrome, with Alzheimer's disease-related pathological features, such as overexpression of Rab5, neflamapimod restored Rab5-GTP+ levels to normal (vs. WT). Neflamapimod-treated animals also had significantly higher numbers of acetyltransferase-positive neurons (P = 0.0037), reduced levels of which are typically associated with basal forebrain neurodegeneration. Neflamapimod also improved performance in the open-field and novel object recognition tests, which are behaviors dependent on basal forebrain cholinergic function. Further, neflamapimod treatment decreased levels of βCTF, the product of APP cleavage by BACE1, which is higher in the transgenic mice than WT due to the reduction of p38α activity and subsequent BACE1 protein expression.

**Clinical Development.** EIP Pharma has completed two Ph. II studies with neflamapimod, one in patients with DLB (NCT04001517; AscenD-LB) and the other one in patients with mild Alzheimer's Disease (NCT03402659; REVERSE-SD). A Ph. II study in Alzheimer's Disease patients (NCT03435861; VIP) is ongoing, while a Ph. II study in patients with Huntington's Disease (NCT03980938) was terminated. Results from the AscenD LB trial showed a significant, clinically-relevant effect size improvement in cognition, as measured by a Neuropsychological Test Battery, in patients who received TID dosing of neflamapimod compared to those receiving the BID dose or placebo.

**Patent.** EIP Pharma has filed two patent applications for neflamapimod. One comprises methods for the treatment of dementia with Lewy Bodies WO2021011432A1, and another for the treatment of gait dysfunction in neurodegenerative disease WO2022099095A1. Neflamapimod was first patented by Vertex (VX-745) WO1998027098A1. However, most patents have already expired, such as US patent US6147080A.

# AZD1390

## ATM kinase

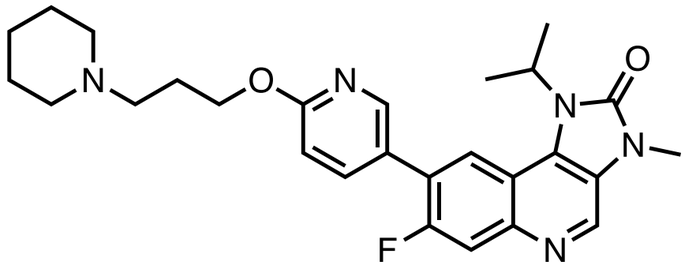


oral ATM kinase inhibitor

Ph. I candidate oncology

biochem-based screen and BBB penetration opt.

*J. Pharmacol. Exp. Ther.*

AstraZeneca, Cambridge, UK

paper DOI: https://doi.org/10.1124/jpet.122.001230

**Context.** AZD1390 (recently published on by University of Minnesota) is a brain-penetrating Ataxia-Telangiectasia Mutated (ATM) kinase inhibitor under development for brain tumors. The kinase, known for its critical role in the repair of lethal DNA lesions induced by radiotherapy treatment, is considered an attractive target for CNS tumors because coupling its inhibition with radiotherapy may lead to radiosensitization of tumor cells. In a recent publication, University of Minnesota scientists investigated the CNS penetration of AZD1390 in mice using transporter knockout models lacking efflux transporters P-gp and Bcrp. Although the compound was found to be an active substrate of P-gp which limited its CNS exposure, effective total concentrations for radiosensitization were still achieved. The compound is currently being evaluated in four Ph. I studies (NCT05182905, NCT03423628, NCT05116254, NCT04550104) in patients with brain tumors and NSCLC, following the completion of another Ph. I study (NCT03215381) in healthy volunteers.

**Target.** ATM kinase is a member of the PI3K kinase family that plays a role in regulating cell cycle checkpoints, DNA repair, and cell survival. Notably, the kinase is a central mediator of the detection, signaling, and repair of DNA double-strand breaks which are lethal DNA lesions induced by radiotherapy or some chemotherapy treatments. This function suggests that combining radiotherapy with inhibition of ATM kinase in tumors may result in radiosensitization.

**Hit-Finding Strategy.** The hit-finding strategy for AZD1390 has not been disclosed.

**Lead Optimization.** The promising pharmacological properties of BBB-penetrating drug, AZD1390, were disclosed. AZD1390 was developed from sames series as first-in-class ATM inhibitor AZD0156, with a focus on brain penetration and kinase selectivity. Although AZD0156 exhibits excellent subnanomolar potency for ATM ($IC_{50}$ = 0.58 nM), it suffers from efflux transporter liabilities leading to poor brain penetration. The tetrahydropyran ring was exchanged with an isopropyl group to reduce the overall polar surface area and the molecular weight, which improved the efflux ratio (no data provided). Installing a fluorine on the bi-aryl ring and substituting a more lipophilic piperidine for the dimethyl amino moiety on AZD1390 improved overall permeability as demonstrated by a low efflux ratio (3.2) in MDCK brain mouse model.

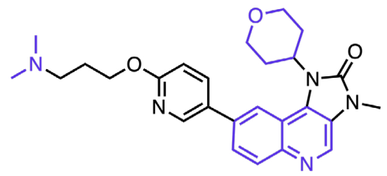


**AZD0156**
ATM cell $IC_{50}$ = 0.58 nM
efflux ratio = 23

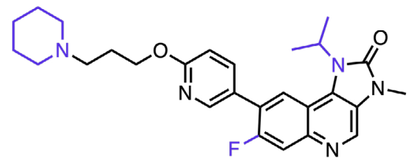


**AZD1390**
ATM cell $IC_{50}$ = 0.78 nM
efflux ratio = 3.2

# AZD1390

## ATM kinase

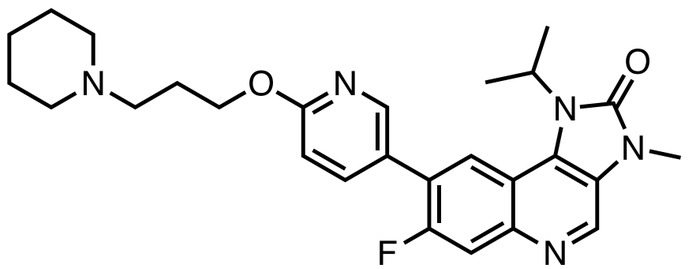

oral ATM kinase inhibitor

Ph. I candidate oncology

biochem-based screen and BBB penetration opt.

*J. Pharmacol. Exp. Ther.*

AstraZeneca, Cambridge, UK

paper DOI: https://doi.org/10.1124/jpet.122.001230

**Lead Optimization.** The promising pharmacological properties of BBB-penetrating drug, AZD1390, were disclosed. AZD1390 was developed from sames series as first-in-class ATM inhibitor AZD0156, with a focus on brain penetration and kinase selectivity. Although AZD0156 exhibits excellent subnanomolar potency for ATM ($IC_{50}$ = 0.58 nM), it suffers from efflux transporter liabilities leading to poor brain penetration. The tetrahydropyran ring was exchanged with an isopropyl group to reduce the overall polar surface area and the molecular weight, which improved the efflux ratio (no data provided). Installing a fluorine on the bi-aryl ring and substituting a more lipophilic piperidine for the dimethyl amino moiety on AZD1390 improved overall permeability as demonstrated by a low efflux ratio (3.2) in MDCK brain mouse model.

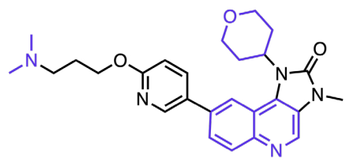

**AZD0156**
ATM cell $IC_{50}$ = 0.58 nM
efflux ratio = 23

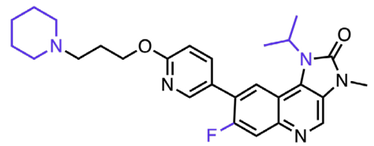

**AZD1390**
ATM cell $IC_{50}$ = 0.78 nM
efflux ratio = 3.2

**Binding Mode.** Not disclosed.

**Preclinical Pharmacology.** AZD1390 is a substrate of the BBB's P-glycoprotein efflux transporter, but despite its reduced penetration, a 20 mg/kg oral dose in glioblastoma mice resulted in a total brain concentration above the in vitro effective concentration (30 nM) needed to achieve radiosensitization. These results are encouraging for AZD1390 as a sensitizing therapy for radiation treatment. Plasma, brain, and spinal cord distribution of AZD1390 after a single oral administration was compared in Bcrp (efflux pump) knockout mice (BKO), P-gp knockout mice (PKO), and a P-gp and Bcrp knockout/ triple knockout mice (TKO), to determine if brain delivery was dependent on on active reflux at the BBB. Brain and spinal cord distribution was highest in TKO mice, although there was significant difference in systemic exposure, clearance, and oral bioavailability between the mouse strains, indicating only limited brain delivery of AZD1390 through active efflux of the BBB. Through steady-state infusion experiments, AZD1390 demonstrated similar distribution across different CNS regions. In a patient-derived xenograft mouse model of glioblastoma, AZD1390 (20 mg/kg) distribution varied according to the tumor region, with the tumor core and rim having higher concentrations that the normal brain, while overall concentrations remained above 30 nM, demonstrating potential radiosensitizing activity.

**Clinical Development.** A Ph. I study (NCT03215381) to analyse brain exposure of [11C]AZD1390 in healthy volunteers has been completed, however findings have not yet been disclosed. The drug is currently being evaluated in four Ph. I studies (NCT05182905, NCT03423628, NCT05116254, NCT04550104) in diseased patients with brain tumors and NSCLC.

**Patent.** The AstraZeneca ataxia telangiectasia mutated kinase inhibitor series was described in the patent WO2017046216A1. The US patent US9856255B2 was granted in January 2018, and is valid until September 2036.

# Upacicalcet

## CaSR

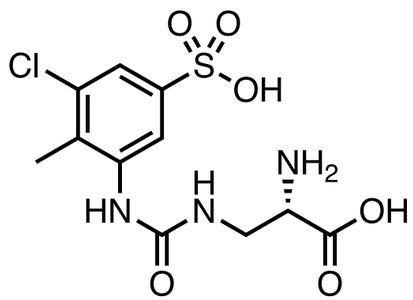


IV CaSR agonist

Ph. III candidate in secondary hyperparathyroidism identified from "kokumi-flavor" studies of peptides

*Mol. Pharmacol.*

Sanwa Kagaku Kenkyusho, Mie, JP

paper DOI: https://doi.org/10.1124/molpharm.122.000522

drug hunter

**Context.** Upacicalcet (Sanwa Kagaku Kenkyusho Co) is a calcium-sensing receptor (CaSR) agonist being developed for secondary hyperparathyroidism (SHPT). The IV drug, first identified in "kokumi-flavor" studies of γ-glutamyl peptides, was approved for SHPT in Japan in 2021 and is currently being developed for the US and other markets. Upacicalcet, like other calcimimetics, acts as a positive allosteric modulator of CaSR and activates the expression of parathyroid hormone. However, unlike the other drugs, such as the widely studied cinacalcet and the recently approved etelcalcetide, upacicalcet has a unique binding method resulting in strong positive allosteric activity. Sanwa Kagaku Kenkyusho scientists believe that this novel binding mode will make the drug a new option for patients whose existing therapies are ineffective, such as those with CaSR polymorphisms.

**Target.** CaSR is a GPCR expressed on the surface of parathyroid cells that regulates extracellular calcium levels by controlling parathyroid hormone (PTH) secretion. CaSR comprises an extracellular calcium-binding domain that senses extracellular calcium levels and a domain that mediates homodimer assembly. Hypercalcemic states result in activation of CaSR, leading to suppression of PTH synthesis, while low calcium levels cause reduced activity of CaSR and hence increased PTH secretion. CaSR loss-of-function mutations have been associated with familial hypocalciuric hypercalcemia type 1, while gain-of-function mutations have been shown to cause autosomal dominant hypocalcemia type 1.

**Mechanism of Action.** Upacicalcet is a positive allosteric modulator of CaSR and is unique in that it competes with l-tryptophan for the amino acid binding site and sensitizes CaSR's $Ca^{2+}$ binding activity. Upacicalcet's mechanism is unlike previous CaSR drugs (e.g., cinacalcet and evocalcet), which are calcimimetic agonists.

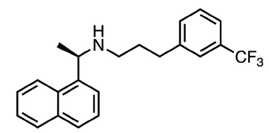


**cinacalcet**

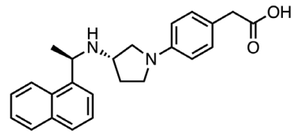


**evocalcet**

**Hit-Finding/Lead Optimization Strategy.** The hit-finding and lead optimization strategies for upacicalcet have not been disclosed.

**Binding Mode.** Although the x-ray crystal structure of upacicalcet in complex with CaSR was not disclosed yet, some insights were provided by docking and MD studies performed by scientists of Sanwa Kagaku Kenkyusho. These studies suggest that upacicalcet interacts with CaSR in the amino acid binding site. That is a different binding mode than previously reported agonists, which usually interact in the seven-transmembrane or extracellular binding domain.

**Clinical Development.** Upacicalcet was approved in Japan in 2021 (Upasita) for patients with SHPT undergoing dialysis. The approval was based partly on a Ph. III study (NCT03801980) in Japanese patients with secondary hyperparathyroidism on maintenance hemodialysis, in which the primary endpoint of mean serum intact PTH (iPTH) level of ≥ 60 pg/mL and ≤ 240 pg/mL from 22 to 24 weeks was achieved in 67% of patients receiving upacicalcet. A long-term extension study is currently underway evaluating the safety and efficacy of the drug during a 52-week treatment period. Recently, Pathalys Pharma, a private late-stage biotech, obtained licensing and commercialization rights for the clinical development of upacicalcet (designated PLS240 for clinical trials) globally.

**Patent.** The patent WO2019124411A1 describes a series of compounds having CaSR agonistic activity for preventing or treating secondary hyperparathyroidism. Under license from EA Pharma, the US patent US11311508B2 was granted in April 2022, and is valid until December 2038.

# CH7057288

**TRK**

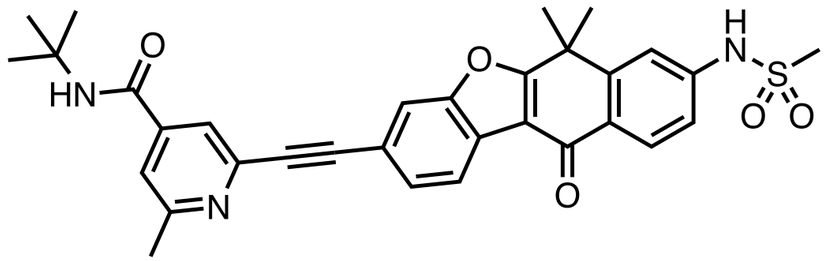

oral pan-TRK inhibitor
tumor regression NIH3T3/NTRK1 mice models
from in-house library screening and SBDD
*J. Med. Chem.*
Chugai Pharmaceutical, Shizuoka, JP

paper DOI: https://doi.org/10.1021/acs.jmedchem.2c01099

**Context.** CH7057288 (Chugai Pharmaceutical Co) is an oral pan-tropomyosin receptor kinase (TRK) inhibitor. Chromosomal rearrangements in the NTRK1–3 genes that encode gene fusions leading to TRK fusion proteins have been shown to drive oncogenesis in many human tumors. Several inhibitors targeting kinase fusions have been developed and are effective for cancers harboring specific fusion oncogenes. Seven of the currently approved kinase fusion inhibitors are tumor-agnostic treatments, two of which target NTRK gene fusion, the pan-TRK inhibitors larotrectinib and entrectinib. In developing CH7057288, Chugai scientists speculated that the strong selectivity for *ALK* and unique scaffold of the highly effective *ALK* inhibitor alectinib could be incorporated to yield a similarly effective pan-TRK inhibitor as a new treatment option for solid tumors with NTRK gene fusions.

**Target.** The NTRK genes, *NTRK1*, *NTRK2*, and *NTRK3*, encode three TRKs (TRKA, TRKB, TRKC, respectively), which are transmembrane receptors that play a role in neuronal development and function. *NTRK* gene fusions have been implicated in various human cancers as oncogenic drivers. For instance, *NTRK* gene fusions involving myosin phosphatase-Rho-interacting protein (MPRIP) and tropomyosin 3 (TPM3) are known oncogenic drivers for non-small cell lung cancer (NSCLC) and colorectal cancer.

**Hit-Finding Strategy.** "Compound 1" was discovered using Chugai's in-house kinase-focused inhibitor library against an 18-kinase assay panel. "Compound 1" is structurally related to the TRK inhibitor alectinib. The tetracyclic hit was atypical of other pan-TRK inhibitors, such as larotrectinib and entrectinib, and was selected as a promising lead for further optimization.

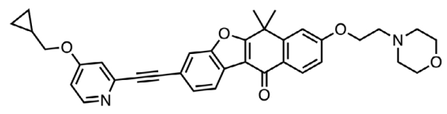

**compound 1**
TRKA $IC_{50}$ = 4.7 nM

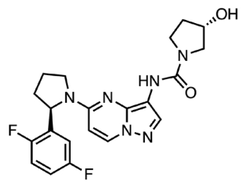

**larotrectinib**

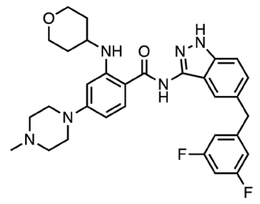

**entrectinib**

# CH7057288

**TRK**

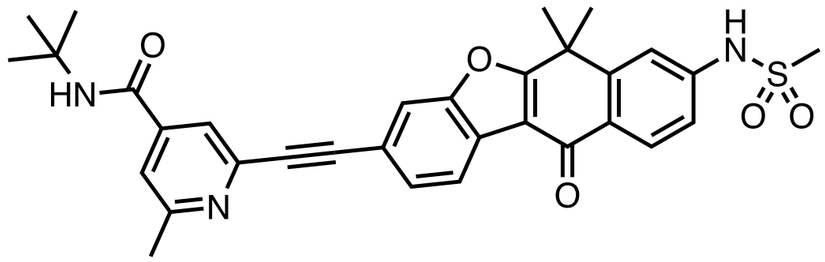

oral pan-TRK inhibitor

tumor regression NIH3T3/NTRK1 mice models

from in-house library screening and SBDD

*J. Med. Chem.*

Chugai Pharmaceutical, Shizuoka, JP

paper DOI: https://doi.org/10.1021/acs.jmedchem.2c01099

**Lead Optimization.** The lead optimization is based on a tetracyclic scaffold, specifically a benzo[b]-carbazole in "compound 1," with a focus on improving inhibitor potency against both TRKA and NIH3T3 MPRIP-NTRK1 (mouse tumor model), while simultaneously mitigating a CYP3A4 induction liability (reported as fold induction vs. DMSO). An empirical ligand-based approach to reduce CYP3A4 induction was employed. PXR activation was not believed to be the mechanism of CYP3A4 induction based on models with PXR. CYP3A4 induction mitigation was achieved by installing a methanesulfonamide at the 8-position in "compound 5d." CYP3A4 activation was effectively reduced (fold induction <2) while potency was maintained.

Further modification of the cyclopropylmethoxy group with a tert-butyl amide and the addition of an $\alpha$-methyl on the pyridine led to the discovery of CH7057288 with improved TRKA potency and selectivity and greater antiproliferative activity in the mouse tumor model line (75 nM vs. 8.4 nM for "compound 5d" and CH7057288, respectively). It should be noted that CYP34A fold induction was found to be higher than 2-fold, but additional testing using an mRNA expression assay with human hepatocytes found no risk of induction with CH7057288 (data not provided).

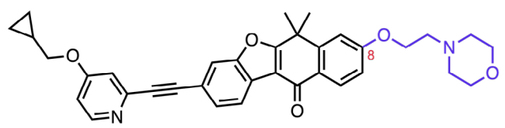

**compound 1**
TRKA $IC_{50}$ = 4.5 nM
CYP34A fold induction = 6.5

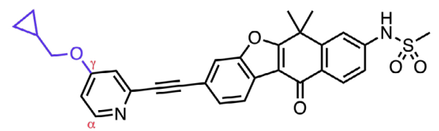

**compound 5d**
TRKA $IC_{50}$ = 3.9 nM
CYP34A fold induction = 1.2

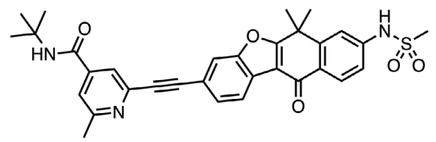

**CH7057288**
TRKA $IC_{50}$ = 1.2 nM
CYP34A fold induction = 3.0

**Binding Mode.** Docking models built by the Chugai scientists suggest that CH7057288 binds to the DFG-out conformation of TRKA as a type II inhibitor. Like alectinib, the ketone of the tetracycle binds to the hinge. They observed CH-$\pi$ interactions between the tetracyclic scaffold and the Val524, Ala542, and Leu516 residues, as well as a hydrogen bond with the hinge backbone NH of M592. The nitrogen in the pyridyl group, considered essential for the TRKA inhibitory activity, as observed in the SAR studies, forms a hydrogen bond with Lys544. Further substitution in the pyridyl ring leads to a decrease in inhibitory activity due to steric clashes with Leu564 and Gly667 residues.

**Preclinical Pharmacology.** ICH7057288 has demonstrated cell growth inhibition against three TRK-fusion positive cancer cell lines, a NSCLC cell line CUTO-3 harboring *MPRIP-NTRK1*, a CRC cell line KM12-Luc harboring *TPM3-NTRK1*, and an acute myeloid leukemia cell line MO-91 harboring ETV6-NTRK3. In mice implanted with NIH313 tumors, CH7057288 (10 mg/kg, PO) significantly inhibited tumor growth, showing 72% tumor regression. In a *MPRIP-NTRK1*-positive NSCLC xenograft mouse model, CH7057288 (10 mg/kg, PO) significantly inhibited tumor growth by 171%. CH7057288 has oral bioavailability of 98% in dog with a $T_{1/2}$ of 15.2 h.

**Clinical Development.** Preclinical compound.

**Patent.** Tetracyclic compounds for the prevention and treatment of NTRK fusion-gene-positive cancers have been described in the patent WO2017073706A1.

# ICeD-2

## DPP9

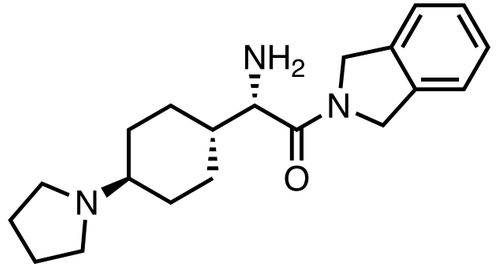


oral DPP9 inhibitor

in vitro synergy with NNRTI for HIV

from 250k cmpd phenotypic screen

*ACS Chem. Biol.*

Merck, Rahway, NJ

paper DOI: https://doi.org/10.1021/acschembio.2c00515

**Context.** ICeD-2 (Merck) is a dipeptidyl peptidase 9 (DPP9) inhibitor under development for HIV-1 infections. Despite the significant advancements in antiretroviral therapy research leading to the approval of some highly effective treatments, the cure for HIV-1 infection has been elusive. A phenotypic screen looking at compound-induced HIV-1 infected cell kill using infected healthy donor PBMCs ultimately led to the tool compound ICeD-2, which was found to inhibit DDP9, an intracellular serine protease.

Notably, the compound synergized with a high concentration of the non-nucleoside reverse transcriptase inhibitor (NNRTI) efavirenz that lowered the effective concentration of ICeD-2 to a clinically relevant dose at a concentration that could not induce total inhibition of DPP9. Complete inhibition of DPP9 is undesirable due to its hypothesized role in mediating apoptosis, proliferation, immune response, among other functions. The tool compound provides proof-of-concept that engagement of the HIV-1 protease activity sensing ability of the CARD8 inflammasome to trigger pyroptosis of HIV-1 infected cells may be worth continuing study for HIV eradication.

**Target.** Target identification experiments including ABPP and CETSA, followed by enzymatic activity and crystallographic confirmation suggested that ICeD-2 targets DPP9, an *N*-terminal dipeptide post-proline-cleaving serine protease that has been studied for its role in the immune system and preadipocyte differentiation. The compound was also found to activate the CARD8 inflammasome, a member of the CARD–containing family of innate immune sensors. The CARD8 inflammasome has been shown to sense HIV-1 protease activity through direct proteolysis of its *N*-terminus by HIV-1 protease. This leads to activation of the inflammasome and subsequent pyroptosis of HIV-1 infected cells. In another study, DPP9 was found to be the restraint protein for CARD8 activation in T cells, suggesting that inhibition of DPP9 and hence CARD8 activation may be a useful therapeutic strategy for HIV-1 infection.

**Mechanism of Action.** ICeD-2 binds to the active site of the DPP9 protease and prevents the assembly of the DPP9/CARD8 (caspase recruitment domain family member 8) ternary complex that sequesters the proteolyzed C-terminal CARD8 fragment from initiating the formation of the inflammasome. Studies showed that DDP9 inhibition led to activation of the caspase recruitment domain family member 8 (CARD8) inflammasome, resulting in pyroptosis of HIV-1 infected cells.

**Hit-Finding Strategy.** The initial hit (CHG-1) was identified from a phenotypic screening workflow using a cell-based assay that monitors loss of GFP expression in cells infected with GFP-tagged HIV-1. A library of 250,000 compounds was assessed using an HIV-infected cell kill assay by monitoring loss of GFP-expressing cells without CTG luminescence (cytotoxicity) reduction, followed by a series of counter screening assays, i.e., removal of non-nucleoside reverse transcriptase inhibitors (NNRTIs), fluorescence interference assay, and a final p24 (HIV-1 capsid protein) secretion assay.

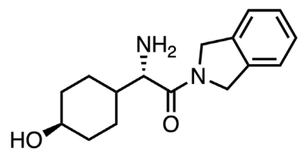


**CHG-1**

GFP $EC_{50}$ = 3615 nM

# ICeD-2

## DPP9

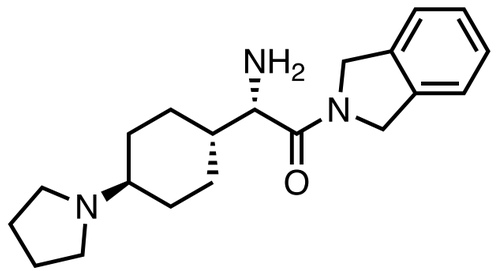


oral DPP9 inhibitor
in vitro synergy with NNRTI for HIV
from 250k cmpd phenotypic screen
*ACS Chem. Biol.*
Merck, Rahway, NJ

paper DOI: https://doi.org/10.1021/acschembio.2c00515

**Lead Optimization.** To enhance the potency of CHG-1, SAR was explored using the same HIV-1 GFP cell kill assay. Among modifications, the primary amine was found to be key to cellular activity, and optimized analogs ICeD-1 and ICeD-2 were synthesized from modular amide coupling and reductive amination, respectively. Both the compounds are potent (GFP $EC_{50}$ = 320 nM, 215 nM) and strongly stabilize DPP9 in a cellular thermal shift assay.

Importantly, ICeD-2 shows excellent selectivity for DPP8 and DPP9 with >3000x fold over DPP4 and DPP7 (biochemical $IC_{50}$ = 3500 nM (DPP4), 3100 (DPP7), 24 (DPP8), 0.9 (DPP9)). Inhibition of DPP4 and 7 has little effect on HIV, but does affect other biological processes. DPP4 inhibitors include the gliptin class of drugs (e.g., sitagliptin) that are involved in glucose homeostasis, and DPP7 has a similar role in metabolic homeostasis. ICeD-2 displayed the desired PK profile (rat IV $T_{1/2}$ = 20 h, $CL_u$ = 75 mL/min/kg, % F = 61). Although these compounds are promising starting points, they were mainly used as tools to deconvolute the mechanism of action of HIV cell killing through DPP9 inhibition.

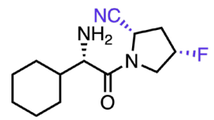


**ICeD-1**
GFP $EC_{50}$ = 320 nM
Biochem $IC_{50}$ = 0.9 (DPP9), 24 (DPP8), 3500 (DPP4), 3100 (DPP7)

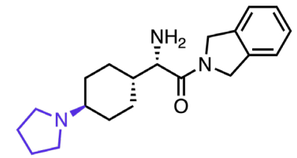


**ICeD-2**
GFP $EC_{50}$ = 215 nM
Biochem $IC_{50}$ = 0.9 (DPP9), 24 (DPP8), 3500 (DPP4), 3100 (DPP7)

**Binding Mode.** The crystal structures of DPP9 bound to ICeD-2 (**PDB:7SVL**) show that the inhibitor bind to the active sites of the proteases. ICeD-2 interacts through hydrophobic and hydrogen bonds involving the carbonyl and the primary amine. These interactions could explain why any modification to the primary amine on the early hit leads to the loss of activity in the HIV-1 GFP cell kill assay.

**Preclinical Pharmacology.** In HIV-1 infected cells co-treated with ICeD-2 and efavirenz, an NNRTI that induces HIV-1-infected cell death through induction of premature intracellular protease activation, a significant increase in HIV-1 cell death (>10x potency and 35% increase in efficacy) was observed compared to each individual agent alone, suggesting a synergistic relationship between DPP9 and the NNRTI.

**Clinical Development.** Preclinical compound.

**Patent.** No publicly available records as of October 2022.

# Vadadustat

## HIF-PHD

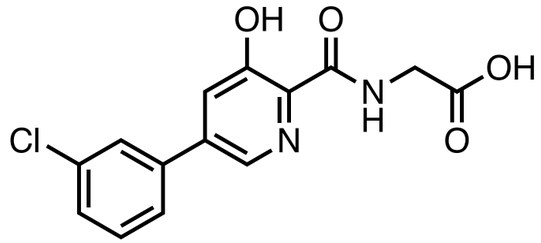


oral HIF-PHD enzyme inhibitor

Ph. III candidate for anemia in CKD

carboxylic acid class of HIF-PHD inhibitors

*J. Pharmacol. Exp. Ther.*

Akebia Therapeutics, Cambridge, MA

paper DOI: https://doi.org/10.1124/jpet.122.001126

**Context.** Vadadustat (Akebia Therapeutics) is an oral hypoxia-inducible factor prolyl-4-hydroxylase domain (HIF-PHD) inhibitor being developed for anemia in patients with chronic kidney disease (CKD). HIFs are transcription factors that mediate the expression of target genes, including for erythropoietin (EPO). In CKD, inhibition of PHDs, a trio of oxygenases, leads to stabilization of HIFs and erythropoiesis, reducing anemia, a significant complication of CKD. The observed effects of the drug on hemoglobin in the clinic, have led to the approval of vadadustat in Japan. However, similar to the previous frontline drug roxadustat (AstraZeneca and FibroGen), FDA concerns about vadadustat's safety have stymied its US approval. In a recent complete response letter, the FDA noted that the data provided do not support a favorable risk-benefit assessment of the drug for dialysis and non-dialysis patients. With the fate of vadadustat in the U.S. is unknown, the search for a U.S.-approved first-in-class oral HIF-PHD treatment for anemia in CKD is still on, although not for long if the planned advisory committee meeting by FDA regulators on GSK's daprodustat goes favorably for GSK.

**Target.** Declining renal function in CKD reduces the ability of the kidney to stimulate erythropoiesis under hypoxic conditions through erythropoietin synthesis, while degradation of HIFs by PHD enzymes (iron-containing 2-oxoglutarate-dependent oxygenases) also reduces erythropoiesis. Therefore, stabilizing HIFs by preventing their PHD-mediated degradation under normoxia to induce mild hypoxic states is an emerging therapeutic strategy for CKD-induced anemia. Five HIF-PHD inhibitors have completed Ph. III trials in the US, but none have been approved, primarily due to concerns over trial length; however, many have been approved/recommended for use in Japan.

**Mechanism of Action.** The treatment for anemia caused by CKD traditionally involved the use of exogenous erythropoiesis-stimulating drugs such as darbepoetin alfa but is associated with cardiovascular risks. As this paper summarizes, the cause of the cardiovascular risks is unclear: "For the specific question about what may be responsible for the excess stroke risk in TREAT, however, all we can say is that there is no smoking gun for now." Vadadustat belongs to a new treatment class that exhibits pan-PHD inhibition and stabilizes the pro-survival transcription factors HIF1-α and HIF2-α, resulting in elevated erythropoiesis, though cardiovascular issues have still been observed with molecules in this class.

**Hit-Finding Strategy.** Vadadustat was first reported by Procter & Gamble in 2008, and was later licensed to Akebia in 2013. Little has been disclosed on its discovery but it possesses similar core elements to other HIF-PHD inhibitors which are derived from 2-OG, a substrate of the target enzyme. Vadadustat is a carboxylic acid-based PHD inhibitor with a monocyclic pyridine core. In the 2013 patent, the in vivo bioactivity of 25 compounds was disclosed out of a total of 576 compounds, including key intermediates and analogs. The 25 compounds have the same monocyclic core with substitutions on the aryl ring and includes methyl ester derivatives, with reports on EGLIN1 (also known as PHD1) and EGLIN 3 (i.e., PHD3) $IC_{50}$ values, vascular endothelial growth factor (VEGF) $EC_{50}$ values, and a yes/no qualitative evaluation of erythropoietic (EPO) response in cells.

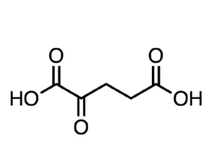


**2-OG**

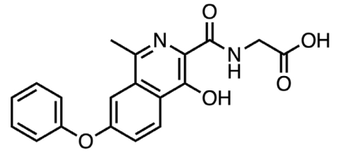


**roxadustat**

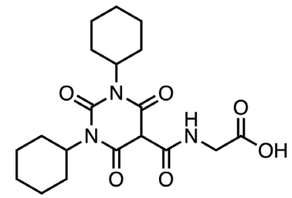


**daprodustat**

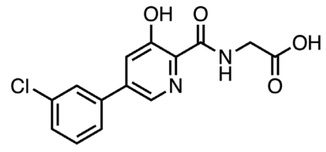


**vadadustat**
PHD1 $IC_{50}$ = 1.1 μM
PHD3 $IC_{50}$ = 0.39 μM

drug hunter

# Vadadustat

## HIF-PHD

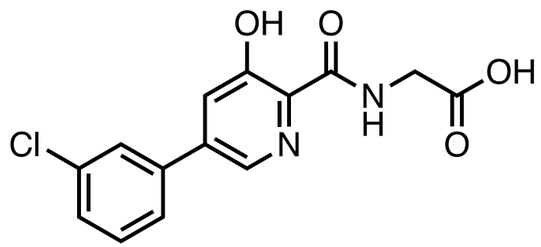


oral HIF-PHD enzyme inhibitor

Ph. III candidate for anemia in CKD

carboxylic acid class of HIF-PHD inhibitors

*J. Pharmacol. Exp. Ther.*

Akebia Therapeutics, Cambridge, MA

paper DOI: https://doi.org/10.1124/jpet.122.001126

**Lead Optimization.** The lead optimization strategy for vadadustat has not been disclosed.

**Binding Mode.** The crystal structure of vadadustat bound with PHD2 isoform (**PDB:7UMP**) shows that the inhibitor occupies the active site. Some of the main interactions displayed in this crystalline structure include bidentate chelation with the iron atom in the active site and a salt bridge with Arg383. The oxygen atom off the pyridyl group interacts with the Tyr303 as a hydrogen bond acceptor and participates in a series of water-mediated interactions.

**Preclinical Pharmacology.** Vadadustat inhibits all 3 human PHD isozymes (1/2/3) and stabilizes HIF-1α and HIF-2α, leading to increased erythropoietin synthesis. Oral dosing of the drug led to a potent increase in erythropoietin levels and a concomitant increase in red blood cell synthesis. Vadadustat increased hematocrit levels in mice, rats and dogs (92%, 68%, and 67%, respectively) and had a similar effect on hemoglobin levels, although with a slight sex effect (81-93%, 54-61%, and 34-39%, respectively). In a 5/6 nephrectomy mouse model of CKD vadadustat dose-dependently increased hemoglobin, hematocrit, reticulocyte count, and mean corpuscular volume, with 90 mg/kg being the most efficacious dose.

**Clinical Development.** Vadadustat has been evaluated in several completed and ongoing clinical trials, with the key studies being the Ph. III PRO$_2$TECT (NCT02648347 and NCT02680574) and INNO$_2$VATE (NCT02865850; NCT02892149) trials. In the PRO$_2$TECT studies the primary endpoint of mean change in hemoglobin concentration during weeks 24-36 and weeks 40-52 was met, however the studies did not meet the primary safety endpoint. Both the safety and efficacy endpoints were met in the INNO$_2$VATE studies.

**Patent.** The patent WO2022150623A1, filled by Akebia Therapeutics, describes vadadustat and other analog compounds for the treatment of several types of anemia. Another patent WO2019028150A1 describes the same compound series for the treatment of hemoglobin disorders.

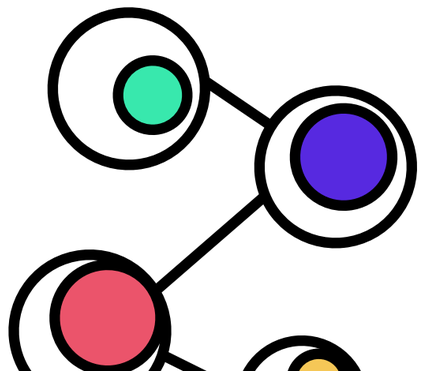

# Small Molecules of the Month

**September 2022**
drughunter.com

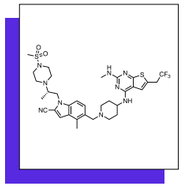

## Ziftomenib | Menin-MLL1 PPI

oral menin-MLL1 inhibitor
Ph. I/II candidate in leukemia
from HTS and SBDD
*Leukemia*
Kura Oncology, San Diego, CA

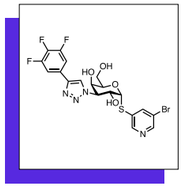

## GB1211 | Galectin-3

oral galectin-3 inhibitor
Ph. I/II candidate in cancer and liver diseases
LLE and PK opt. from a prev. clinical candidate
*J. Med. Chem.*
Galecto Biotech, Gothenburg, SE

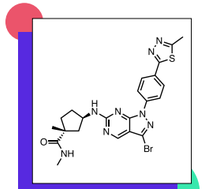

## Compound 39 | GCN2

oral GCN2 kinase inhibitor
TGI in LL2 syngeneic mouse model
SAR opt. from literature starting point
*J. Med. Chem.*
RAPT Therapeutics, South San Francisco, CA

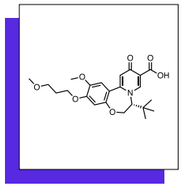

## GST-HG131 | PAPD5/PAPD7

oral HBV antigen inhibitor
Ph. I candidate for hepatitis B
SAR opt. of a previously disclosed inhibitor
*Bioorganic Med. Chem. Lett.*
WuXi AppTec, Shanghai, CN

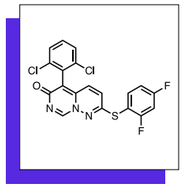

## Neflamapimod | p38α kinase

oral p38α kinase inhibitor
Ph. II candidate in neurology
from SBDD and opt.
*Nat. Commun.*
EIP Pharma Inc, Boston, MA /
Vertex, Cambridge, MA

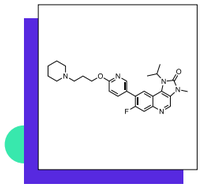

## AZD1390 | ATM kinase

oral ATM kinase inhibitor
Ph. I candidate oncology
biochem-based screen. and BBB penetration opt
*J. Pharmacol. Exp. Ther.*
AstraZeneca, Cambridge, UK

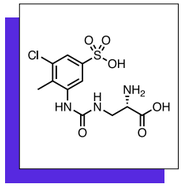

## Upacicalcet | CaSR

IV CaSR agonist
Ph. III candidate in secondary hyperparathyroidism
identified from "kokumi-flavor" studies of peptides
*Mol. Pharmacol.*
Sanwa Kagaku Kenkyusho, Mie, JP

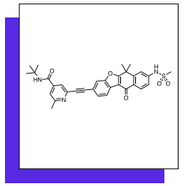

## CH7057288 | TRK

oral pan-TRK inhibitor
tumor regression NIH3T3/NTRK1 mice models
from in-house library screening and SBDD
*J. Med. Chem.*
Chugai Pharmaceutical, Shizuoka, JP

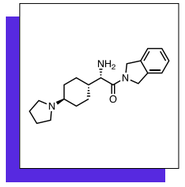

## ICeD-2 | DPP9

oral DPP9 inhibitor
in vitro synergy with NNRTI for HIV
from 250k cmpd phenotypic screen
*ACS Chem. Biol.*
Merck, Rahway, NJ

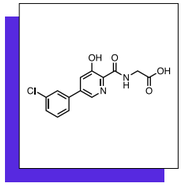

## Vadadustat | HIF-PHD

oral HIF-PHD enzyme inhibitor
Ph. III candidate for anemia in CKD
carboxylic acid class of HIF-PHD inhibitors
*J. Pharmacol. Exp. Ther.*
Akebia Therapeutics, Cambridge, MA

# discover together

drughunter.com
info@drughunter.com